Space Weather Studies Using Ground-based Experimental Complex in Kazakhstan

O.Kryakunova[1], A.Yakovets[1], C.Monstein[2], N.Nikolayevskiy[1], B.Zhumabayev[1], G.Gordienko[1], A.Andreyev[1], A.Malimbayev[1], Yu. Levin[1], N.Salikhov[1], O.Sokolova[1], I.Tsepakina[1]

[1]Institute of Ionosphere, NCSR, Kazakhstan;
[2]Institute for Astronomy, Swiss Federal Institute of Technology Zurich (ETHZ), Switzerland

E mail (krolganik@yandex.ru).

Abstract Kazakhstan ground-based experimental complex for space weather study is situated near Almaty. Results of space environment monitoring are accessible via Internet on the web-site of the Institute of Ionosphere (http://www.ionos.kz/?q=en/node/21) in real time. There is a complex database with hourly data of cosmic ray intensity, geomagnetic field intensity, and solar radio flux at 10.7 cm and 27.8 cm wavelengths. Several studies using those data are reported. They are an estimation of speed of a coronal mass ejection, a study of large scale traveling distrubances, an analysis of geomagnetically induced currents using the geomagnetic field data, and a solar energetic proton event on 27 January 2012.

Keywords: space weather, bursts of solar radio emission, Callisto radio spectrometer, geophysical database.

1. Introduction

Space weather is conditions on the Sun and in the solar wind, magnetosphere, ionosphere and thermosphere that can influence the performance and reliability of space-borne and ground-based technological systems and can endanger human life or health. So, space weather research is very important for all countries. The science of space weather is focused in two distinct directions: fundamental research and practical applications. Kazakhstan is promoting researches in these areas with an international collaboration.

2. Experimental Setups and Database

In Kazakhstan there is an experimental complex for space weather study. It includes an experimental setup for records of cosmic ray intensity by using a neutron monitor (Zusmanovich, Kryakunova and Shepetov, 2009), a magnetic observatory at Alma-Ata, an optical interferometer called the Spectral Airgrow Temperature Image (SATI) instrument for observing the emission of night sky, an ionospheric sounder, a solar radio telescope for the measurements of the solar radio flux at frequencies of 1.078 GHz (27.8 cm) and 2.8 GHz (10.7 cm) with 1-second time resolution, and a Callisto radio spectrometer (type eC37) (Zhantayev et al., 2014). All data are presented on the web site of the Institute of Ionosphere (http://www.ionos.kz/?q=en/node/21) in real time. Almaty Cosmic Ray station is a part of the worldwide neutron monitor network and contributes to the real-time database for high resolution neutron monitor mesurements called the NMDB (www.nmdb.eu) in Europe. Geomagnetic observatory at Alma-Ata (43.18 N, 76.95 E) is certified as a station of the International Real-time Magnetic Observatory Network called the INTERMAGNET (www.intermagnet.bgs.ac.uk) and has provided its data. Alma-Ata data have been sent to the Dcx-index Server in University of Oulu, Finland (http://dcx.oulu.fi) in real-time for calculation of Dcx-index (corrected and extended Dst-index) since 2010.

Now we have a complex database with hourly data of cosmic ray intensity, geomagnetic field intensity and solar flux at 10.7cm and 27.8 cm wavelengths. An example of data plots by the Kazakhstan ground-based experimental complex is presented in Figure 1. The measurements by means of Kazakhstan experimental complex are presented in Figure 1.
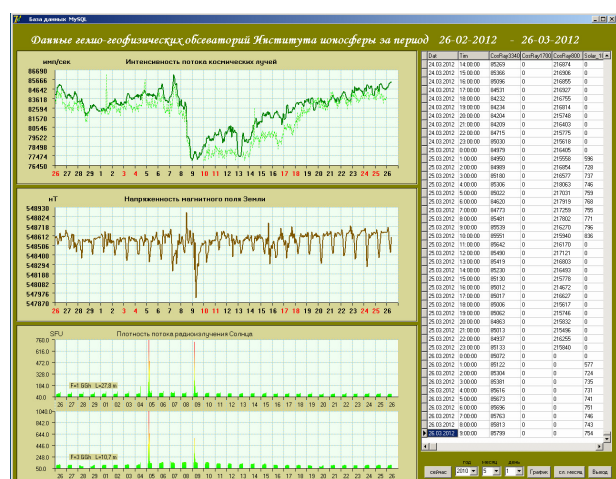

Figure 1. An example of data plots using real-time data of the Kazakhstan ground-based experimental complex.

The SATI instrument developed in Canada (http://stpl.cress.yorcu.ca/SATI) was installed at the experimental base area of the Institute of Ionosphere at Orbita near Almaty at 2730 m altitude above sea level in 2007. By measuring the column emission rate and vertically averaged rotational temperature of the OH (6–2) and of the O2 (0–1) atmospheric band, the SATI instrument monitors the atmospheric temperature at about 87 and 95 km where the peaks of the OH and O2 emission layers are located, respectively. The SATI is based on the property of a narrow-band Fabry–Perot interference filter that transmits light from spectral lines of decreasing wavelength at increasing incidence angles (see Figure 2). In the SATI instrument, the etalon is used as a narrow band interference filter and a CCD camera is used as a detector. Figure 2 shows an example of an observed gravity wave with the following parameters: the period of the first wave mode is 80-90 minutes and the horizontal speed of the wave is 80-100 km/h.
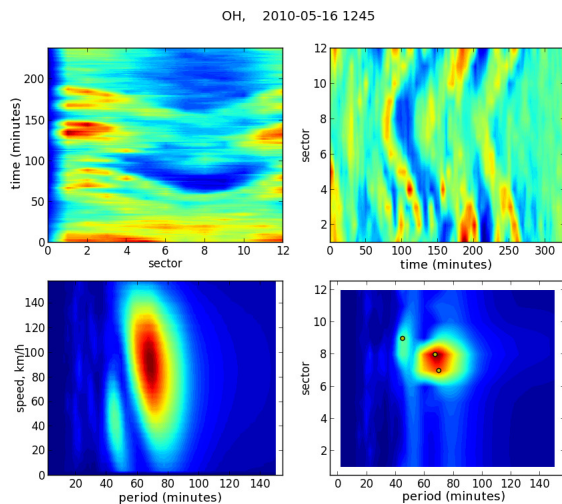

Figure 2. An example of wave structures in the OH emission observed by the SATI instrument.

3. Recent Scientific Results

3.1 Estimation of speed of a coronal mass ejection (CME)

We realized a method for measuring the speed of CMEs based on spectrographic observations of type II solar radio bursts (fundamental frequency slowly drifting towards lower frequencies) generated by the shock wave originated from the CME (Gopalswamy, 2012; Pohjolainen et al., 2007; Vršnak et al., 2001). A burst recorded in the 24-th cycle of solar activity on the radio spectrograph Callisto installed at Almaty is analyzed. An estimation of speed of a CME using the standard model (Manchester et al., 2004) of the altitude dependence of the coronal plasma density is carried out.

Figure 3 shows the dynamic spectrum of a type II burst observed on 8 January 2014. There was a splitting of the fundamental frequency, which began in 03:47 UT at frequency $f \approx 230$ MHz and ended at 03:52 UT at

a frequency of ≈ 110 MHz. Time derivative of the fundamental frequency was $df / dt \approx 0.40$ MHz / s and a scale height calculated from the plasma frequency of 170 MHz corresponds to $h \approx 1.17$ Rs. The average speed is estimated as $v \approx 415$ km/s.
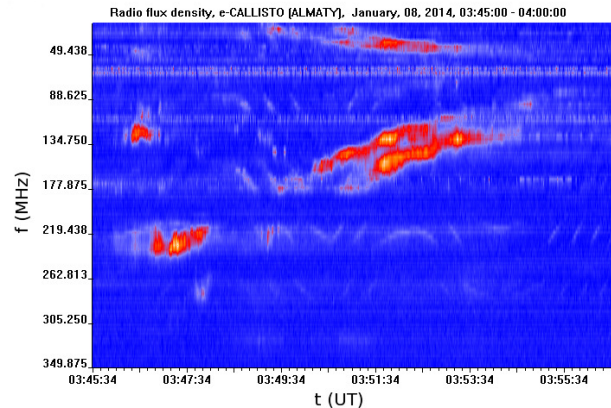

Figure 3. The dynamic spectrum of the type II burst recorded on 8 January 2014.

3.2 Observation of large scale traveling ionospheric disturbances (LSTIDs)

Space weather specification and forecasting require proper modeling which account for the regular features of magnetosphere, thermosphere and ionosphere. Geomagnetic storms strongly affect ionosphere. LSTIDs caused by the strong geomagnetic storms are a part of "space weather event chains" which originate in solar atmosphere and end in Earth's atmosphere. Internal atmospheric gravity waves (AGWs) also play an important role in dynamics of space weather. On the basis of theoretical and experimental investigations, several models have been developed to describe the main characteristics of AGW-LSTID relationship on a global scale. These models reflect the level of understanding of the basic physical principles governing the atmospheric and ionospheric processes and can be permanently improved by new experimental data incorporated in the model calculations. Our study considers reaction of thermospheric wind and ionospheric F2-layer on the propagation of AGWs exited by geomagnetic storms. Nighttime observations of LSTIDs in F2-layer have been performed at the Institute of Ionosphere (Almaty, 76°55 E, 43°15 N) by using a digital ionosonde. The nighttime observations were selected for the LSTID analysis because the LSTIDs with large amplitudes of variations in ionospheric parameters, substantially exceeding the accuracy of the virtual heights h'(t) and critical frequencies f_oF_2 reading from ionograms, are observed at midlatitudes mainly at night. The data processing included obtaining temporal variations in the electron content N(t) for fixed altitudes and variations of altitudes of the F-layer maximum h_mF, bottom $h_{bot}F$ and half-thickness Δh and critical frequency f_oF (see Figure 4). The 1166 night observation sessions were carried out during the analyzed period, and 581 nights were characterized by wave activity with the rage of period more than 60 minutes. Variations of N(t) for series of

altitudes allowed us to define an altitude corresponding to peak amplitude of the LSTID.

AGWs at midlatitudes have a wavelength often exceeding 1000 km. For such a wave, the motion of the neutral gas at heights of F-layer presents a horizontal wind blowing equatorward along the meridian during the passage of one half wave over the observation point and northward during the passage of the subsequent half wave over this point. Ionospheric F-layer plasma is involved into the motion due to the collisions of neutrals with ions. The plasma in F2-layer is magnetized and therefore can move only along the magnetic flux tubes. This motion is driven by the neutral wind component directed along the magnetic field. The neutral wind blowing equatorward and poleward pushes plasma along the magnetic field lines upward and downward, respectively, resulting to periodical oscillations in F-layer peak altitude. Knowing the magnetic dip angle (for Almaty $I = 62°$) it is easy to estimate an amplitude of the meridional wind oscillations (V_m and V_{mb}) from the peak-to-peak amplitudes ($\Delta\ h_mF$ and $\Delta\ h_{bot}F$) of h_mF and $h_{bot}F$ oscillations. Typical examples presented in Figure 5 demonstrate that during observation sessions several waves with slightly different amplitudes and periods occurred. Variations of electron density $N(t)$ at a series of altitudes are shown in the top panels. Variations of altitudes of the F2-layer maximum h_mF and the F2-layer bottom $h_{bot}F$ are shown in the second top panels. In order to eliminate the trend caused by a diurnal component of meridional wind (towards the equator at night) a high-frequency filtering was performed using second-degree polynomial. Filtered h_mF variation are shown in the third top panel. Filtered $h_{bot}F$ variation are shown in lower panel (see Figure 5).
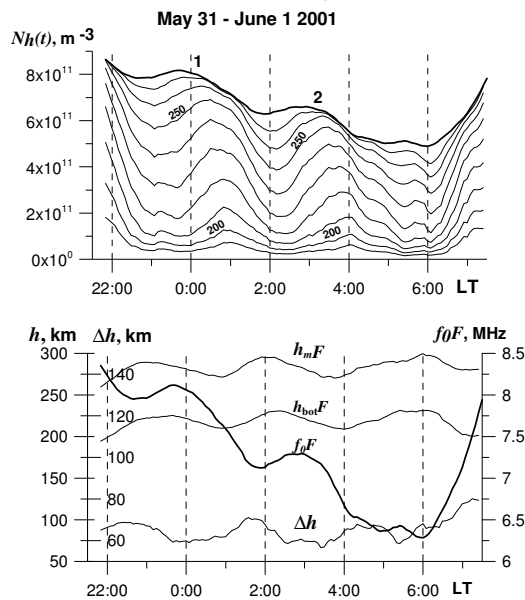

Figure 4. Variations of F-layer parameters calculated from altitude profiles: a) electron density $N(t)$ at a series of altitudes with the distance between the adjacent altitudes of 10 km interval (top panel), b) altitudes of the F-layer maximum h_mF, bottom $h_{bot}F$, half-thickness Δh and critical frequency foF (bottom panel) during LSTID passage.
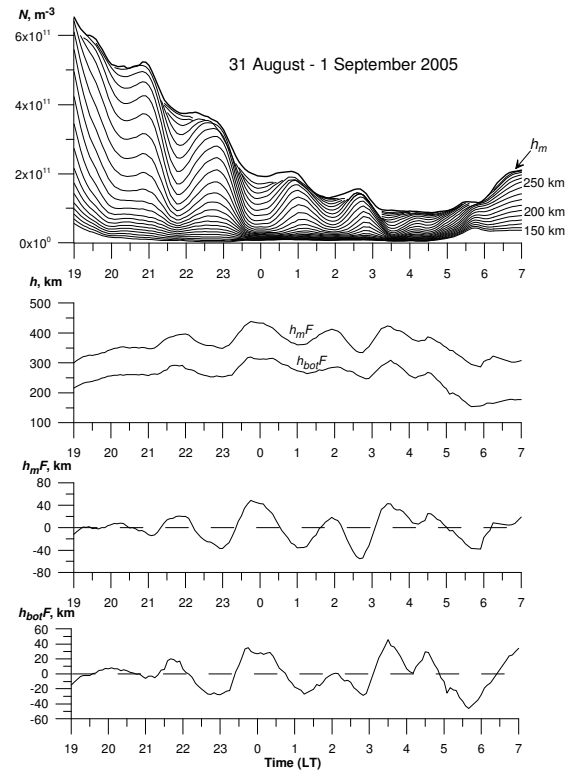

Figure 5. Examples of variations of F-layer parameters: a) electron density $N(t)$ at a series of altitudes with the distance between the adjacent altitudes of 10 km interval (top panel), b) altitudes of F-layer maximum h_mF and F-layer bottom $h_{bot}F$ (the second top panel), detrended h_mF (the third top panel), detrended $h_{bot}F$ (bottom panel).

3.3 Analysis of geomagnetically induced currents (GICs) using geomagnetic field observation data

Appearance of GIC in conductive ground-based systems such as power lines and pipelines is one of the negative effects of space weather on technological systems. GIC flows in main power lines through a neutral of high-voltage transformers, subsequently passing through transformer windings and coming into phase conductors of a power line. Until recently, it has been considered that intense GICs flow in power systems located in auroral zones. Therefore, most studies have been performed for high latitudes. However, Koen and Gaunt (Koen and Gaunt, 2002) cited the cases of large GICs at midlatitudes. Therefore, the problem of GICs seems to be possible in Kazakhstan where the total length of the network of high-voltage (220–1150 kV) power lines is about 27000 km. The aim of the present work is to study a possibility of appearance of considerable GICs in this region based on the variations in the horizontal component of geomagnetic feild measured at Alma-Ata (AAA), Novosibirsk (NVS), and Irkutsk (IRT) magnetic observatories, the geomagnetic latitudes of which are close to those of the Kazakhstan southern and northern borders.

The method used in our studies is based on the linear dependence between GIC and time derivative of the horizontal component of magnetic fields dH/dt, following from the Faraday law. Initial data for this

study were the minute values of the variations in the X and Y components of the magnetic fields at AAA and NVS and the horizontal component H and declination D of the magnetic fields at IRT (see Figure 6).

During seven periods of high magnetic activities in 2003–2005, we determined the durations with large time derivatives of geomagnetic field exceeding the threshold of 30 nT/min when GIC could cause unwanted consequences in the power grids in Kazakhstan. We noted that the Kazakhstan power systems have a possibility to be affected by considerable GICs for rather long time periods during strong storms (especially during the storm of October 30–31, 2003).

We demonstrated that large dH/dt values responsible for significant GIC values were observed at a sudden commencement of strong storms, which is a impulsive variation of the geomagnetic fields, and during large-amplitude pulsations of the geomagnetic fields.

We constructed the distributions of the dH/dt and dH/dt directions. The most interesting properties are narrow distributions of H and dH/dt extended along the magnetic meridian at AAA and wider angular distributions at NVS and IRT (see Figure 7).
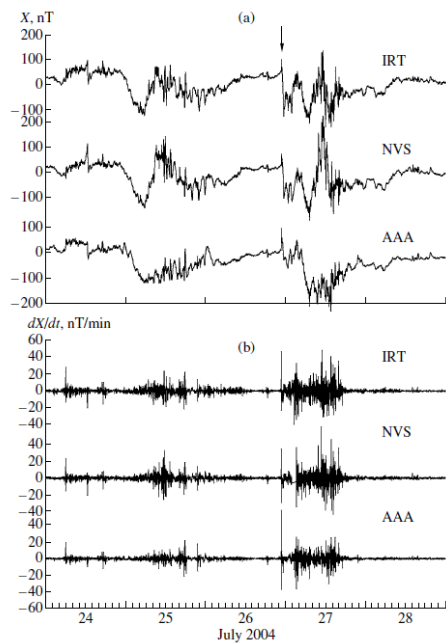

Figure 6. Variations (a) of the northern component and (b) time derivative for three observatories during the magnetically active period between 24 and 28 in July 2004.
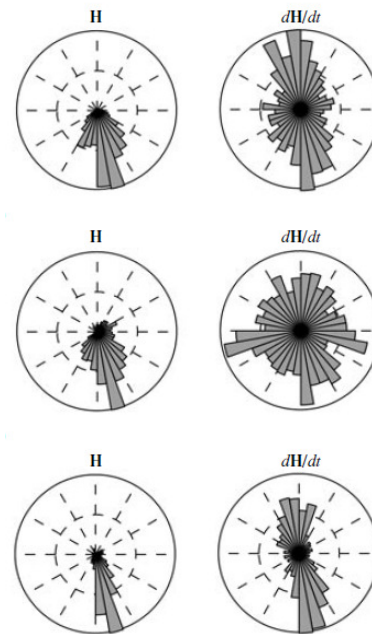

Figure 7. Distributions of H and dH/dt directions for Irkutsk (top panels), Novosibirsk (middle panel) and Alma-Ata (lower panel) in the magnetically active period between 24 and 28 in July 2004.

3.4 Ground level enhancement (GLE) on 27 January 2012

Currently, it is considered that in the 24th cycle of solar activity, only 2 ground level enhancements (GLEs) of solar energetic particles were obserevd on 17 May 2012 and on 6 January 2014. The number of solar proton events (SPEs) observed by the GOES satellites are much higher than the number of GLEs on the ground. GLEs tend to ocurr associated with larger events which cause considerable radiation impacts. Approxymately 30 solar proton events were observed in 2012. We decided to analyze the behaviour of the cosmic ray intensity recorded by the world wide neutron monitor network during the events of the 24th solar activity cycle when a significant increase of the integral proton flux with energy more than 100 MeV was recorded by the GOES satellites. GLE should be considered an event when at least one NM at sea level shows a statistically significant increase of count rate coinciding with an increase of the satellite observation. However, nobody paid attention to an ocurrence of GLEs associated with small SPEs.

The first large proton event in 2012 started on 23 January after the M8.7 flare from the active region AR11402 (N27W71), located at western side of solar disk. The particle flux with energy more than 100 MeV was 2.3 pfu. On 24 January, the flux of particles with energy more than 10 MeV reached 3400 pfu (radiation storm of level 3 by the NOAA/SWPC space weather scale: http://www.swpc.noaa.gov/sites/default/files/images/NOAAscales.pdf) and on 25 January, the flux became 6300 pfu (radiation storm of level 2). On 26 January, the

proton enhancement continued with the radiation storm of level 1. The next enhancement ocurred by the X1.7 flare on 27 before the previous event finished. The source of this flare was in the same active region AR11402 (N27W71) which by this time came to the western limb of the visible solar disk. At 17:27 UT on 27 January in this active region, the X1.7 flare occurred and reached maximum at approximately 18:37 UT (peak time). Time of the CME lift-off was 18:28 UT. Type II radio burst started at 18:30 UT. At this time a large inclease of proton flux with energies more than 10 MeV (800 pfu), 50 MeV (50 pfu), and 100 MeV (11.9 pfu) occurred. For the particles with energy more than 100 MeV, the event was close to background level on 28 January 2012. For particles with energies more than 10 MeV, the event lasted much longer and finished on 1 February 2012.

In Figure 8, the data from the NMs at South Pole B (SOPB), South Pole (SOPO) and Alma-Ata B (AATB) with a time resolution of 10 minutes (baseline time interval is 17:00 – 18:00 UT on 27 January) are plotted together with the 5-minute GOES 13 data for protons with energies more than 10 MeV, 50 MeV, and 100 MeV, respectively.

On 27 January 2012, an increase of the counting rate of ~2%, at polar NMs coincided with the increase of integrated proton flux recorded by the GOES satellite (E>100 MeV). Such an increase is also recorded at several sea level NMs. Those data suggests that this event is a small GLE.
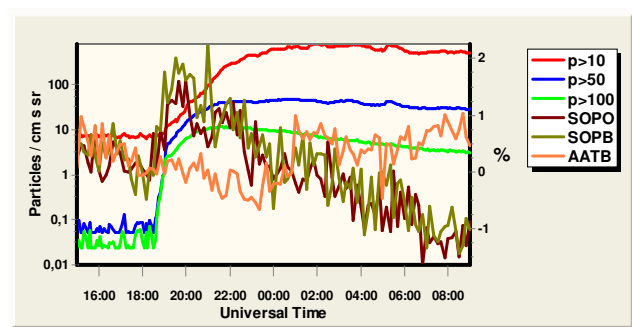

Figure 8. Cosmic ray variations (right scale) recorded at NMs South Pole B (SOPB), South Pole (SOPO), and Alma-Ata B (AATB) with 10-minute resolution and 5-minute data of proton fluxes recorded by GOES 13 between 15:00 UT on 27 January 2012 and 09:00 UT on 28 January 2012.

4. Summary

The measurements of key parameters of space weather in real time at the Kazakhstan ground-based experimental complex are available on the Institute of Ionosphere web-site (http://www.ionos.kz/?q=en/node/21). Seneral analysises using the Kazakhstan ground-based experimentaal compex data are presented. Now we plan to develop an information acquisition system of experimental geophysical data with high temporal resolution and an information center to keep the experimental geophysical data. It is intended to include the measurements of cosmic ray intensity, Earth's magnetic field, density of solar radio-emission, and new measurement data such as secondary gamma-radiation and thermal neutrons into the general MySQL database.

References

Gopalswamy, N.: 2012, ISWI workshop, Quito, Ecuador.

Koen, J. and Gaunt, CT.: 2002, Abs. The 27 general Assembly of URSI, Netherlands, Maastrich, 177.

Manchester, W.B.IV, Gombosi, T.I., Roussev, I., Ridley, A., De Zeeuw, D.L., Sokolov, I.V., Powell K.G., and To´th, G.: 2004, J. Geophys. Res., 109, A02107.

Pohjolainen, S., van Driel-Gesztelyi, L., Culhane, J.L., Manoharan, P.K., and Elliott, H.A.: 2007, Solar Physics, 244, 167.

Vršnak, B., Aurass, H., Magdalenič, J., Gopalswamy, N.: 2001, Astron. Astrophys., 377, 321.

Zhantayev, Zh., Kryakunova, O., Nikolayevskiy, N., and Zhumabayev, B.: 2014, Sun and Geosphere. 9(1-2), 71.

Zusmanovich, A.G, Kryakunova, O.N., and Shepetov, A.L.: 2009, Advances in Space Res. 44, 1194.